Marine and Petroleum Geology 28 (2011) 1047–1060

Contents lists available at ScienceDirect

Marine and Petroleum Geology

journal homepage: www.elsevier.com/locate/marpetgeo

1000 m long gas blow-out pipes

Helge Løseth [a,*], Lars Wensaas [a], Børge Arntsen [b], Nils-Martin Hanken [c], Christophe Basire [d], Knut Graue [e]

[a] Statoil ASA Research Centre, Arkitekt Ebbels veg 10, No-7005 Trondheim, Norway
[b] Department of Petroleum Engineering and Applied Geophysics, Norwegian University of Science and Technology, S. P. Andersens veg 15, No-7491 Trondheim, Norway
[c] Department of Geology, University of Tromsø, No-9037 Tromsø, Norway
[d] Statoil ASA EPN ONO ASG PTC SMB, Strandvegen 4, No-7500 Stjørdal, Norway
[e] Statoil ASA INT-GEX SA EA, Drammensveien 264, No-0283 Oslo, Norway

ARTICLE INFO

Article history:
Received 27 April 2010
Received in revised form
27 September 2010
Accepted 14 October 2010
Available online 18 November 2010

Keywords:
Blow-out pipe
Gas leakage
Nigeria
Rhodes
Seismic interpretation
Seabed crater
Outcrops of blow-out pipe
Seismic modelling
Hydro fracturing

ABSTRACT

This study presents seismic observation of pipe anomalies from offshore Nigeria, outcrops of blow-out pipes from Rhodes, Greece, and geophysical modelling of an acoustic pipe. The studies give insight into how pipes form, their internal structure, the seismic image and geophysical artefacts related to the pipes. Over one hundred seafloor craters, 100 m–700 m wide and up to 30 m deep, have been observed on the seafloor offshore Nigeria. They are underlain by interpreted cones and seismic pipe anomalies that can be traced down to reservoir zones at 1000 m–1300 m below the seafloor. The seismic pipe anomalies are 50 m–150 m wide and almost vertical. They are interpreted as up-scaled pipes found in outcrops on Rhodes, Greece. The outcrops show pipe-related structures at three levels. Lowest, the reservoir rock contains metre-sized cavities which are filled with a mixture of clay derived from the overlying cap rock. In the middle, several circular to oval structures in plane view of pipes are observed in the lowest part of the cap rock. Highest, 15 m into the clay cap rock, strongly sheared country rock forms circular structures with a core of structureless clay. Based on outcrop observation on Rhodes we constructed an acoustic model of a 50 m wide and 1000 m long pipe. Seismic modelling proves that such pipes would be expressed in seismic data, that they are similar to the seismic pipe anomalies offshore Nigeria but this study also revealed that prominent intra-pipe reflections are artefacts. A formation model for the pipes is suggested: High fluid overpressure in the reservoir generated hydro fractures from the reservoir to seafloor where a mixture of gas and fluid flowed at high speed to form pipes, cones and seafloor craters. After hours to weeks of gas and fluid flow through the pipe the pore pressure in the reservoir dropped and the blow-out terminated. Muddy slurry fell back and plugged the cavity in the reservoir and the pipe.

1. Introduction

Direct observations of hydrocarbon leakages are difficult for the obvious reason that they take place below the Earth's surface. Evidence of the active leakage of oil or gas and associated formation water is therefore most commonly found on the surface, on the seafloor or in seawater (Cartwright et al., 2007; Deville et al., 2006; Evans et al., 2008; Graue, 2000; Hovland and Judd, 1988; Heggland and Nygaard, 1998; Leifer et al., 2006; Løseth et al., 2009; Mazzinia et al., 2008), while remnants of subsurface palaeo-leakage anomalies may be found in the outcrops (Parnell and Kelly, 2003; Deville and Mascle, in press; Cobbold et al., 1999). Active subsurface leakage is generally only imaged indirectly, e.g., by seismic or by other remote subsurface imaging tools or observation in well cores or wireline logs (Revil and Cathles, 2002). Seismic images provide the most extensive available indications of leakage, and several interpreted leakage anomalies are reported in the literature (Cartwright et al., 2007; Deville et al., 2006; Evans et al., 2008; Graue, 2000; Heggland and Nygaard, 1998; Løseth et al., 2009; Mazzinia et al., 2008).

Pipe-shaped seismic anomalies were observed in a 3D seismic dataset from deep water offshore Nigeria by Løseth et al., (2001). A cluster of seafloor craters and underlying sub-vertical pipe-like structures were observed and described. Similar pipe-like

* Corresponding author. Tel.: +47 48125621.
E-mail addresses: heloe@statoil.com (H. Løseth), lawe@statoil.com (L. Wensaas), borge.arntsen@ntnu.no (B. Arntsen), nils-martin.hanken@uit.no (N.-M. Hanken), cba@statoil.com (C. Basire), graue@statoil.com (K. Graue).

0264-8172/$ – see front matter © 2010 Elsevier Ltd. All rights reserved.
doi:10.1016/j.marpetgeo.2010.10.001

anomalies are later observed in seismic data from several places around the world (Bünz et al., 2003; Cartwright et al., 2007; Moss and Cartwright, 2010a,b; Trincardi et al., 2004). The shapes of seafloor crates, pipes as well as intra-pipe reflections have been described in detail and various formation processes have been suggested (Moss and Cartwright, 2010a and b; Hustoft et al., 2007, 2010). Generally, pipes form a high-permeable vertical zone, also called a 'seal bypass system' (Cartwright et al., 2007), where fluids and gas can be transported faster than would otherwise be allowed by the normal permeability in the pore network of the sediments. Pipes, mud volcanoes, sand injections and gas chimneys are all types of bypass structures. High fluid overpressure opening a hydro fracture through low permeable sediments is a common first phase of all these bypass structures (Arntsen et al., 2007; Cartwright et al., 2007; Løseth et al., 2009; Rodrigues et al., 2009).

Even with the very best seismic data quality available today, such data will only give a very simplified acoustic impedance contrast picture of the real rock shapes and internal structures. Therefore, seismic anomalies must be related to known leakage processes or outcrop structures before they are interpreted. We have studied outcrops of palaeo-pipe structures on Rhodes, Greece. These provided insight into the rocks and structures formed during leakage and the processes taking place within vertical pipe structures, the surrounding host rock and the underlying reservoir. We postulate that the pipes exposed on Rhodes were similar in shape and process to the pipe anomalies observed on seismic data offshore Nigeria. Therefore an up-scaled acoustic model of an outcrop pipe was constructed and an artificial seismic 2D line was shot across the pipe in order to compare these seismic images with that of pipe anomalies offshore Nigeria.

In this paper we describe details of the seismic pipe anomalies, outcrops of palaeo-pipes from Rhodes, compare synthetic seismic images of an associated up-scaled acoustic model with the seismic pipe anomalies offshore Nigeria and propose a formation model for the pipes.

1.1. Geological setting

The main study area is located in the western part of the southern lobe in the Niger Delta (Fig. 1). The Niger Delta is more than 10 km thick and is a prolific hydrocarbon province. It comprises Eocene to Recent sediments of the Akata, Agbada and Benin formations (Doust and Omatsola, 1989; Morgan, 2003). The Akata Formation, comprising deep water parallel-laminated marine muds, is 3–4 km thick and is considered the principal source rock (Doust and Omatsola, 1989; Haack et al., 2000). The Upper Miocene to Recent Agbada Formation is 2–9 km thick, comprises mixed clastic sediments which is the main hydrocarbon reservoir rock and the host of the pipes. The Benin Formation is mainly continental and fluvial in origin. Mud volcanoes have been observed in the western lobe of the Niger Delta (Graue, 2000). Fluid vents have also been observed in anticlinal structures in the outer

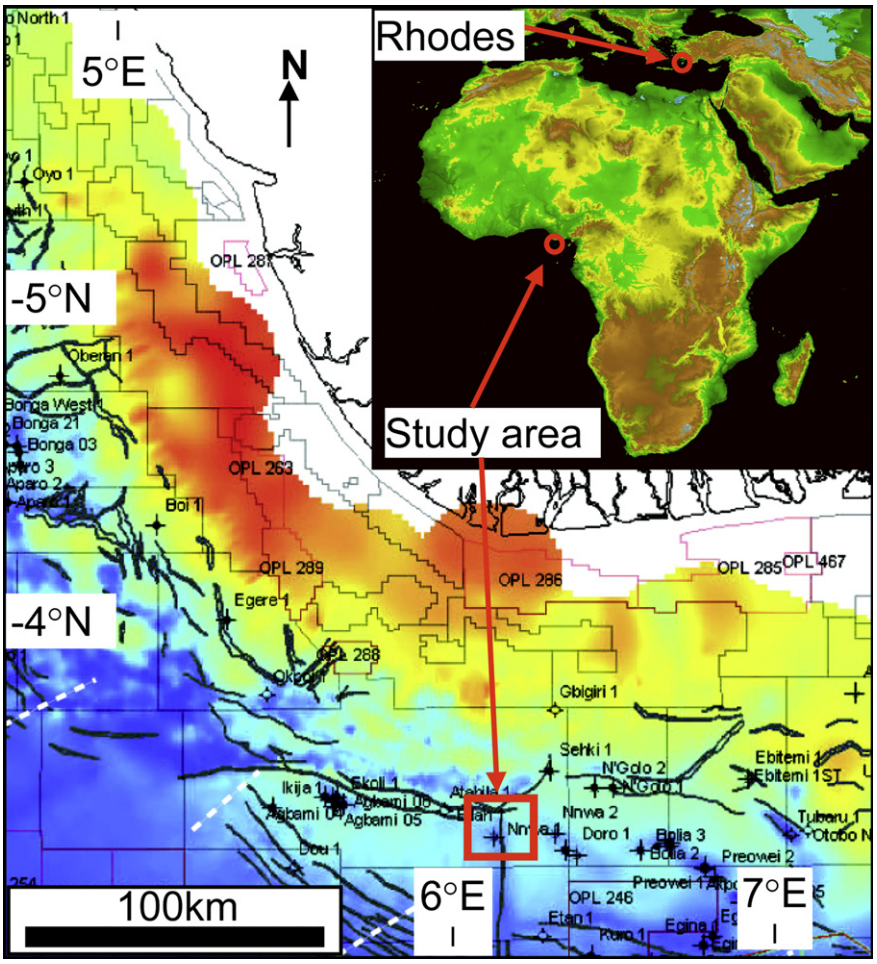

Fig. 1. The main study area (red square) is located in the offshore part of the Niger Delta at water depths between 1100 m and 1350 m. It is located just south of the southernmost of the E–W striking inner trust faults and is bisected by a N–S strike-slip fault. Colours show thickness of Agbada Formation (dark red = 9 km, dark blue = 2 km). The study area on Rhodes is also indicated.

trust belt (Cobbold et al., 2009). They are most likely sourced from the severely overpressured Akata Formation (Cobbold et al., 2009). The study area is located above a dome structure penetrated by the Bilah-1 well. The dome is located just south of the southernmost part of the E–W striking fault in the inner trust belt (Figs. 1 and 2) and is bisected by a N–S striking strike-slip fault (Fig. 3). The strike-slip fault branches upward from a single fault at depth to several NNE–SSW striking en-echelon normal faults that indicate left-lateral fault movement. Both the strike-slip fault and the reverse fault are considered active as the seafloor is offset or bulged along the faults (Figs. 2 and 3). A cluster of near circular depressions is observed on seafloor at water depths between 1100 m and 1350 m above a mapped structural 4-way closure (Fig. 2).

2. Seismic observations

A 400 km^2 area of a larger 3D dataset has been studied. Well tie shows that an increase in acoustic impedance coincides with peak reflection expressed as black-blue colour on 0-phase migrated data. The near, full and far trace data, which are shown in most seismic figures, have been rotated 90° so an increase in acoustic impedance falls on zero-crossing from black-blue to red-yellow. Various seismic cubes were available. The near trace data (2–16°) appear to give the most distinct expression of the pipe anomalies and are therefore frequently used in this paper (Fig. 4).

2.1. Seafloor craters

About 110 large seafloor craters are clustered above an N–S elongated dome-shaped structural closure (Figs. 2 and 3). The cluster of craters covers approximately 60 km^2. The craters are circular to semi-circular and vary from 100 m to 700 m in diameter. Most of the larger craters are between 200 m to 600 m in diameter (Figs. 5 and 6). The smaller craters appear V-shaped on seismic sections, while the larger craters vary between V-shape, two high-dip sides and a relative flat base, and an asymmetric shape with one high-dip side and one low-dip side. Bright amplitude anomalies are observed at the base of a few of the craters (Fig. 5d and e). The spacing of individual craters is irregular but some depressions overlap, making the recognition of individual craters difficult. Individual craters can be up to 30 m deep, but most craters are between 15 m and 25 m deep. The volume of the missing sediment mass in the craters, assuming a pre-crater seafloor that follows the regional seafloor, is between 5×10^6 m^3 and 2×10^6 m^3 for a crater of 500 m diameter and 30 m depth, and 0.6×10^6 m^3 and 0.2×10^6 m^3 for a crater of 200 m in diameter and 20 m depth.

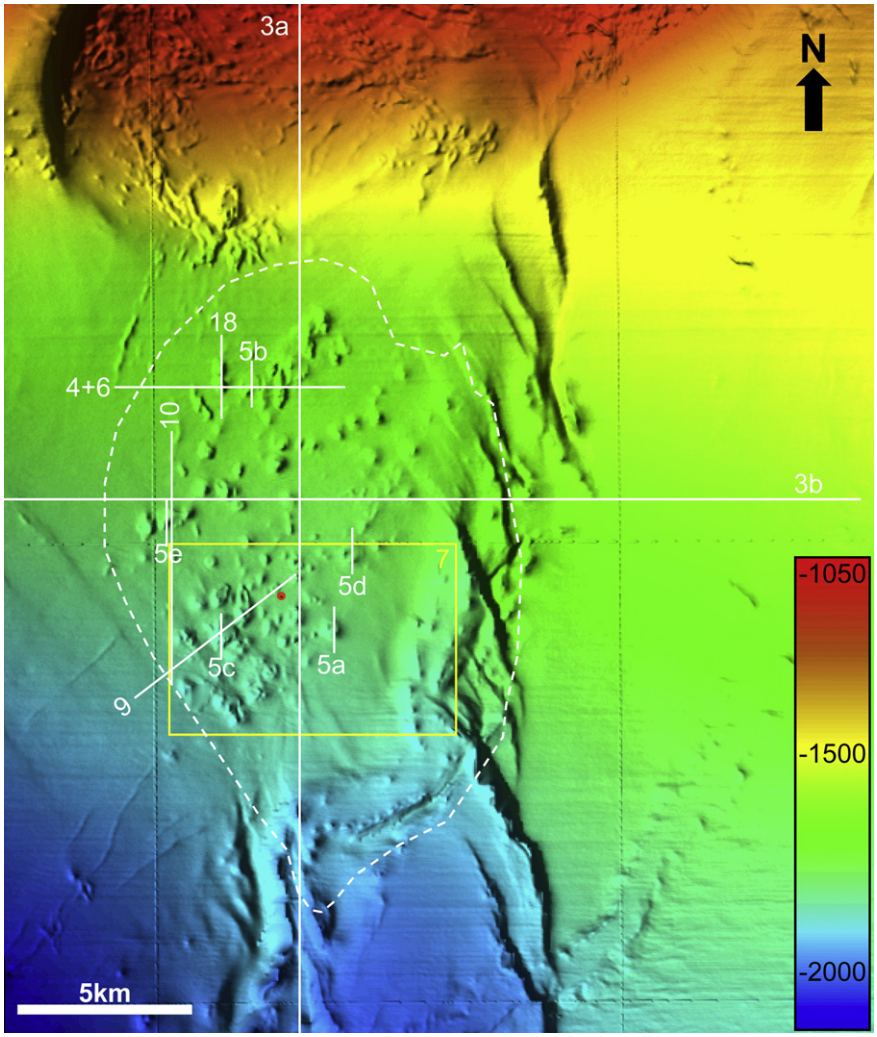

Fig. 2. Seafloor map from 3D seismic data lightened from E (depth in milliseconds). Circular to semi-circular seafloor craters are clustered within an approximate 60 km^2 area. The craters are mainly located above a structural closure 1000 m below seafloor (white dotted line). The en-echelon faults offsetting the seafloor suggest a left-lateral strike-slip fault movement. Locations of the seismic lines in the following figures are shown. The red dot shows the location of the Bilah-1 well.

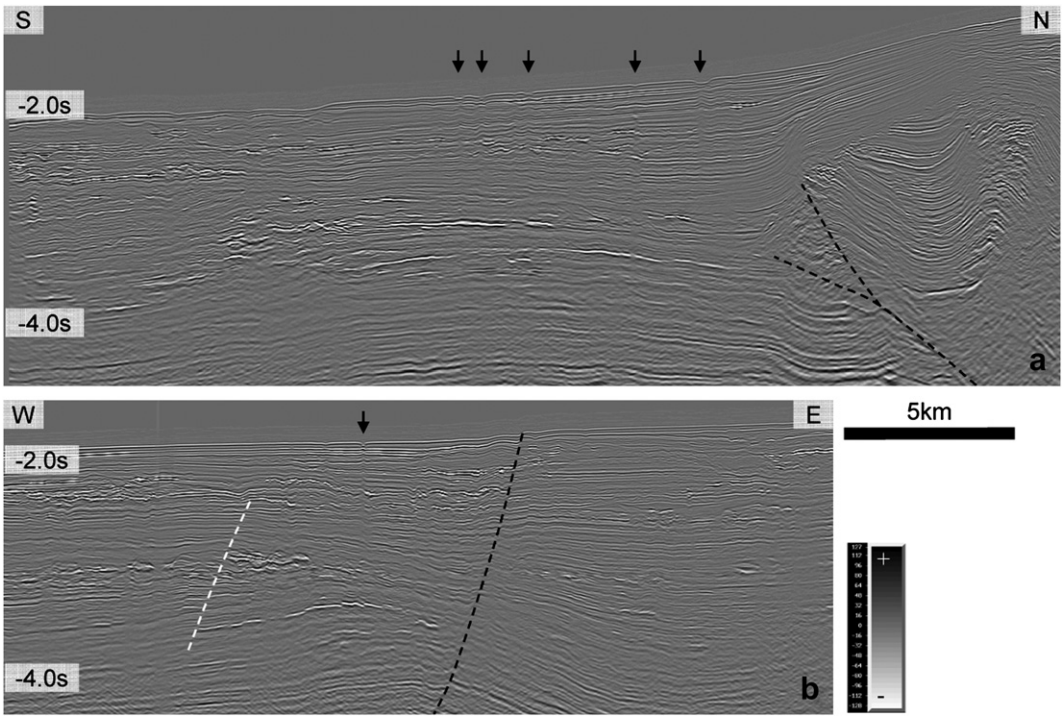

Fig. 3. The N–S (a) and E–W (b) seismic sections show the dome structure at depths below 3.0 s. Both the southward moving trust fault and the N–S striking main fault are interpreted (black dotted line). Both faults are interpreted to be active as seafloor is either offset or flexured. Seafloor craters (black arrows) and underlying vertical pipe anomalies can be seen. Location in Figure 2.

2.2. Cones

Cone shaped zones are interpreted below several of the larger craters (Figs. 5 and 6). The correct way of interpreting the cone boundary is not obvious but we have chosen to place it at the discontinuity of the reflections outside the cone. Interpreting the same cone on various seismic cubes, we find our preferred interpretation changing with the processing (Fig. 6b). The conical zone varies from one anomaly to the next but is approximately 60 m deep below a typical 300 m wide and 22 m deep crater (Figs. 5 and 6b). The flanks of the cone are dipping approximately 30° towards the centre. At the base of the cone, the reflections from the layered sequence outside the anomalies continue into a tiny anticline with a vertical central zone comprising distorted seismic

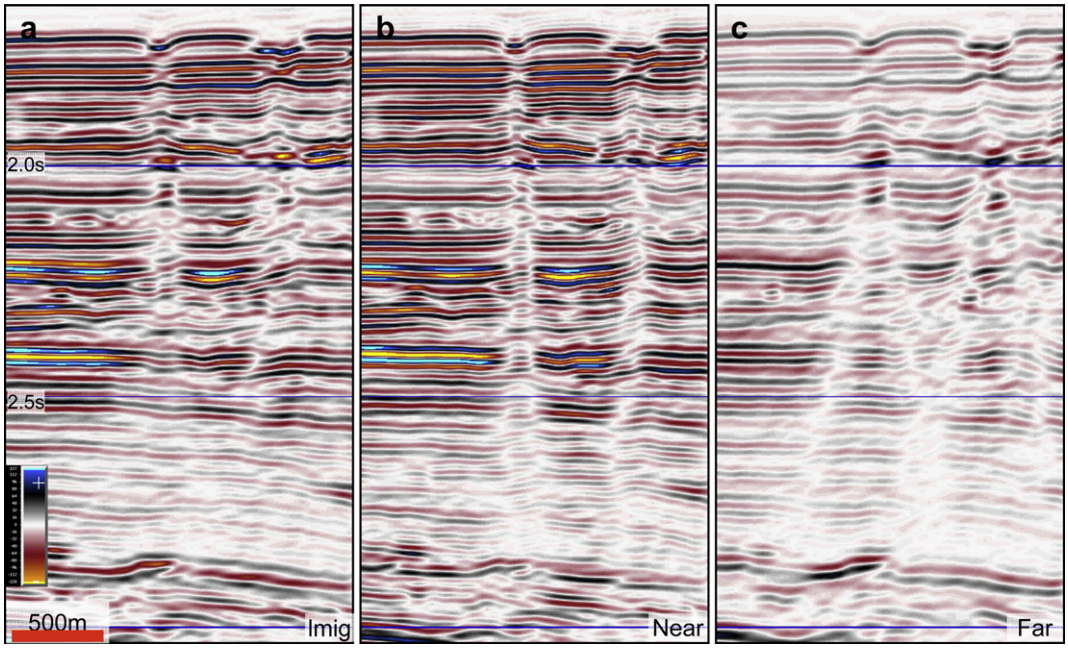

Fig. 4. Seismic expression of seafloor craters and pipe anomalies on a) full, b) near and c) far trace data. The pipe anomalies have the most distinct expression on the near trace data. On the far trace data the pipe anomalies appear to split into two discontinuity zones below 2.2 s. The pipe anomalies that can be observed below 2.5 s on near trace data appear to be smoothened out on full stack data. Location in Figure 2.

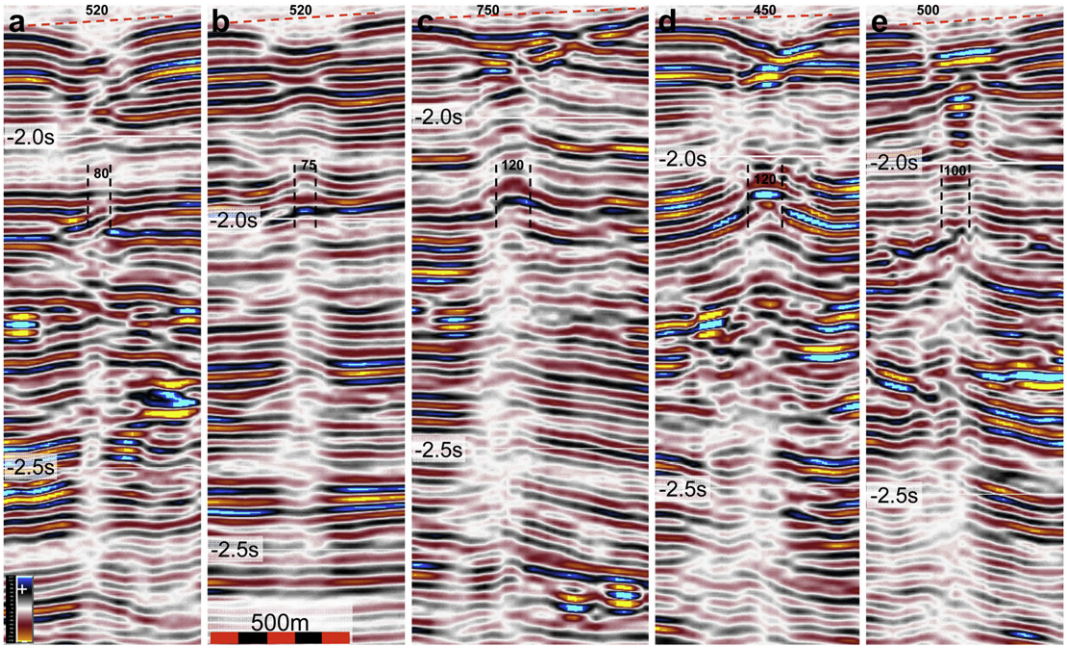

Fig. 5. Figure 5a–e show various expressions of seafloor craters and underlying pipe anomalies. The interpreted horizontal width of the craters is indicated with the red dotted line. Bright amplitudes can be observed in the seafloor crater in Figure 5c, d and e. Generally, the pipe anomalies become more diffuse towards the depth. Dotted black lines show the interpreted width of the pipe anomalies. Location in Figure 2.

signals (Figs. 5 and 6). The centre of the anticline is often cut by one or two vertical, fault-like discontinuities.

2.3. Vertical pipe anomalies

Near vertical zones with distorted seismic signals are found below the seafloor craters and underlying cones (Figs. 5 and 6). Generally, the distorted zone has a circular to oval shape on time slices and a pipe shape in 3D. Various seismic reflection patterns are observed in the distorted zone. Often the central zone comprises a short distance reflection with a similar dip to those outside, but laterally a polarity shift can be observed inside compared to that outside (Figs. 5d, e and 6). The pipe anomalies also comprise continuous reflections across the pipe but with local anticlines (Figs. 5c and 6). Most commonly the pipe anomalies comprise dimmed reflection with variable continuity (Fig. 5). The transition from the dimmed reflections and the outside stratigraphic reflections becomes more diffuse with depth. Together these anomalies stack on top of each other to define pipe-shaped anomalies which are circular to elliptic on time slices (Fig. 7). The pipe anomalies vary from vertical to sub-vertical and locally cut in and out of vertical seismic sections (Fig. 8). The boundaries between the pipe anomalies and the surrounding stratigraphic reflections are most precisely imaged in near trace data and are interpreted where the outside stratigraphic reflections either lose continuity or where they dome up to form local anticlines (Fig. 4). The diameter of the pipe anomalies varies from 50 m to 150 m. Far from all pipe anomalies reach the seafloor (Fig. 9). The upper terminations of the pipe anomalies are interpreted where the overlying stratigraphic related reflections continue across them without disturbance.

The 3D shape of the pipes was difficult to image using conventional seismic data. Therefore a 3D-visualisation program (gOcad) and an internally developed algorithm were used to extract the shape. This was done by manually picking the centre of the crater on the seafloor. From this starting cell the algorithm moved automatically one cell down in a coherency-like attribute cube and searched all the neighbouring horizontal cells. For each down step, a new cell with the minimum coherency value was identified and kept as the new starting point. The process continued until the bottom of the seismic cube was reached. All the selected cells are stored into a point-set visualised as thin lines (Fig. 8).

We traced some of the pipe-like dim zones 1000 m–1300 m below the seafloor into elongated bright amplitudes, which are interpreted as deep marine reservoir sands. The pipes are interpreted to be rooted here (Figs. 8 and 10). The bright amplitude reservoir zone is segmented by faults that strike NNW–SSE and dip between 45° and 60°. In a few places, it is possible to observe that the near vertical pipe anomalies cut through fault planes (Fig. 9). They also cut across bright amplitudes which are interpreted as deep marine sands (Fig. 10). In Figure 8 the reservoir units are connected by the pipes to the seafloor craters.

3. Outcrop studies from Rhodes, Greece

Vertical pipe-like structures have been observed within Late Pliocene to Pleistocene clay at Cape Vagia on the northeastern side of the Greek island of Rhodes (Hanken et al. 1996; Løvlie and Hanken, 2002). These pipe-like structures are believed to represent small scale outcrop analogues to the pipe-shaped seismic anomalies offshore Nigeria. Rhodes and the Rhodes Basin to the east are located on the Aegean-Antolian microplate, which is limited to the south by the subducting African plate (Hall et al., 2009). The Aegean-Antolian microplate is tectonically active and has gone through a complex tectonic evolution with significant vertical movements during the Neogene (Hall et al., 2009). The entire eastern Aegean-Antolian microplate was exposed during the Messinian and a regional unconformity developed. In northeastern Rhodes this unconformity separates karstified Mesozoic marble from an overlying isolated outlier of Pliocene – Pleistocene sediments (Hanken et al., 1996; Cornée et al., 2006a). The studied pipes are found in one of the outliers situated at Cape Vagia (Fig. 11). The lower parts of the pipe-related structures are located in shallow marine limestones termed the Kolymbia Limestone of Pliocene age (Hanken et al., 1996; Løvlie and Hanken, 2002). The pipes extend

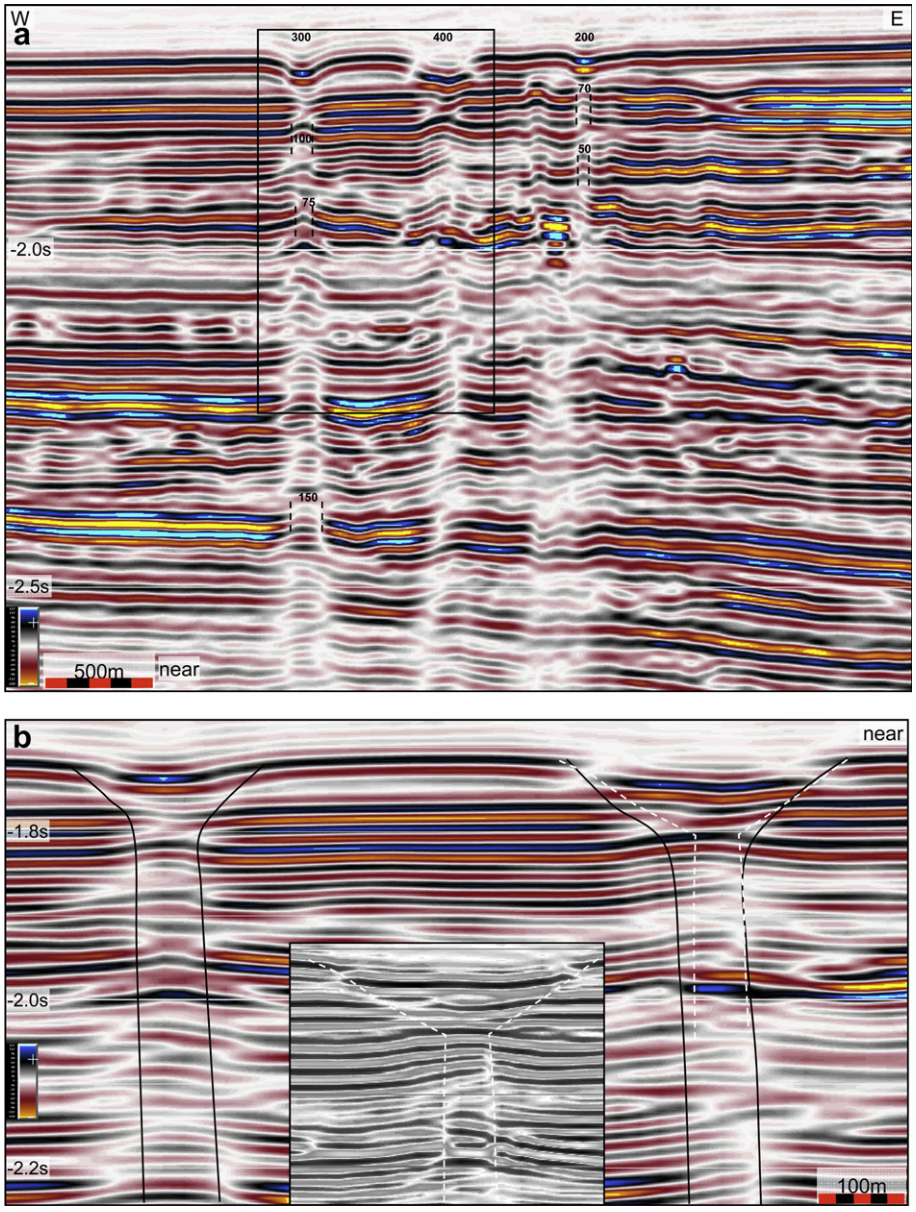

Fig. 6. a) Seismic expression of three craters on the seafloor where funnel-shaped cones are interpreted below the two largest. The underlying pipe anomalies are interpreted at the discontinuous boundary between the intra-pipe anomalies and the outside continuous reflections that are best expressed in the westernmost pipe anomaly. Some of the reflections can be traced continuously across the pipe where they describe an anticline. The middle pipe anomalies are defined by a combination of vertical stacked anticline domes and one-sided discontinuous reflection. Stacked tiny anticlines define the seismic pipe anomaly below the small easternmost pipe. The frame shows the location of the approximately 1:1 scale expression of the pipes in Figure 6b). The boundary between outside reflections and the intra-funnel and pipe is interpreted. The insert in Figure 6b) shows an old processing of the same line and preferred funnel and pipe interpretation. When this interpretation is superimposed on the near trace data (white dotted line) the difference between the two preferred interpretations becomes clear. However, it is uncertain which interpretation is the most correct. Location in Figure 2.

through the 15 m high coastal sections of the overlying pelagic Lindos Bay clay member of the Rhodes Formation but the original height of the pipes is not known as the upper part is eroded. A volcanic layer in the Lindos Bay clay has been dated in another of these Pliocene – Pleistocene outliers to 1.89 ± 0.09 Ma (Cornée et al., 2006b). The area subsided from above sea level during the Pliocene to around 500 m water depth before it was uplifted again (Hanken et al., 1996; Cornée et al., 2006a). A total of 41 pipe-related structures have been observed in the study area in the Cape Vagia outlier. They crop out at three stratigraphic levels (Fig. 11):

1) Lowest: The pipe-associated structures occur in the upper part of the Kolymbia limestone, a highly porous and permeable, calcareous, and moderately cemented reservoir grainstone (Fig. 12). On the shore face we observed small areas where the grainstone has been replaced by mud and mud clasts from the overlying Lindos Bay clay and grains from the carbonate sand (Fig. 12). The cavity which is up to 6 m long, 2 m wide and 3–4 m high has a semi-3D exposure due to the local topography. The stratigraphic lowest part can be traced down to the underlying metamorphosed limestone and the upper tip goes into a pipe-like structure in the Lindos Bay clay. The transition between the infill and the surrounding grainstone host rock is sharp. No fractures are observed in the country rock. Several circular structures that are nearly 1 m in diameter are part of the clay filled cavity. Here, a second generation of clay has filled the circular structures and has connecting 20 cm wide fracture-like zones (Fig. 12b).

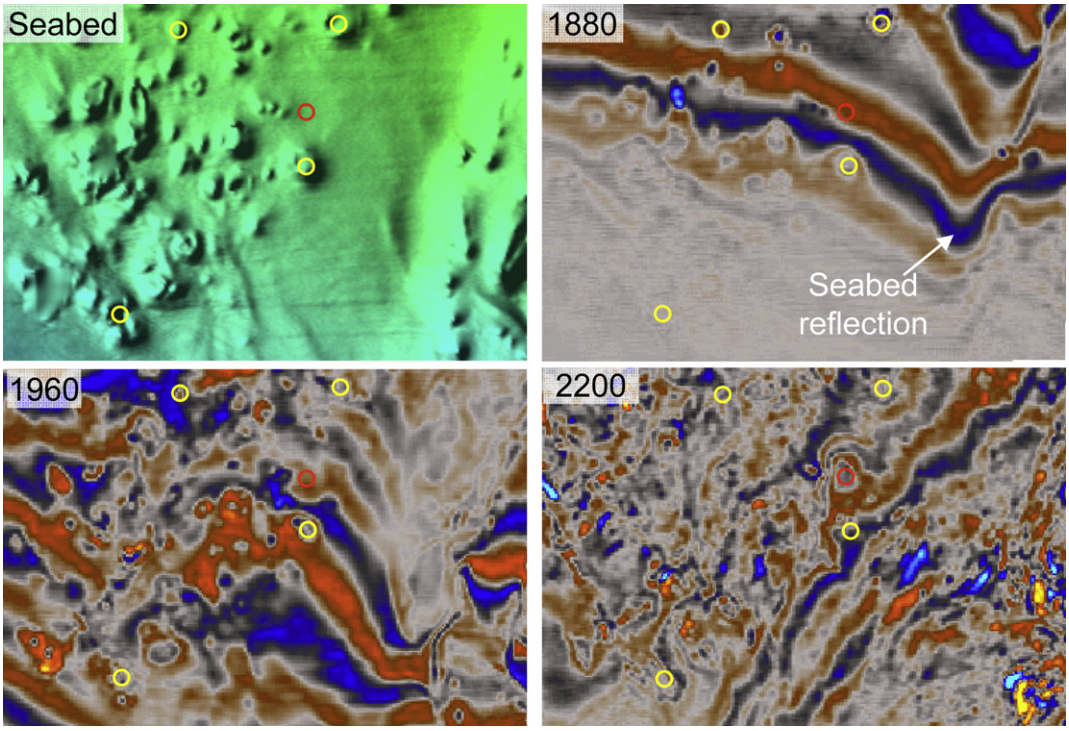

Fig. 7. a) Seafloor with craters and underlying time slices of seismic data at 1880 ms, 1960 ms and 2200 ms. The pipe anomalies have circular to semi-circular expressions on the time slices. The yellow circles show four craters which are interpreted on seafloor and superimposed on the time slices. The red circle shows a circular anomaly interpreted on the 2200 ms time slice. An associated seafloor crater is not observed on the seafloor and this anomaly is therefore interpreted as a palaeo-pipe. Location in Figure 2.

2) Middle: The boundary between the Kolymbia limestone and the overlying Lindos Bay clay coincides with an erosion-formed terrace in the terrain (Fig. 11). The Lindos Bay clay is a cap rock clay with average grain size of 6–9 phi and TOC of 0.1–0.2%. It is so soft that it can be cut with a knife and has been used for pottery. Several circular to oval plane view pipe exposures can be studied along this terrace. One of the best exposed pipes in the lowermost part of the Lindos Bay clay consists of a central pipe with sub-concentric fractures (Fig. 13). The fractures typically dip ~80° away from the core and extend up to 10 m horizontally from the centre of the pipe. The spacing between the individual vertical fractures increases from less than 5 cm, close

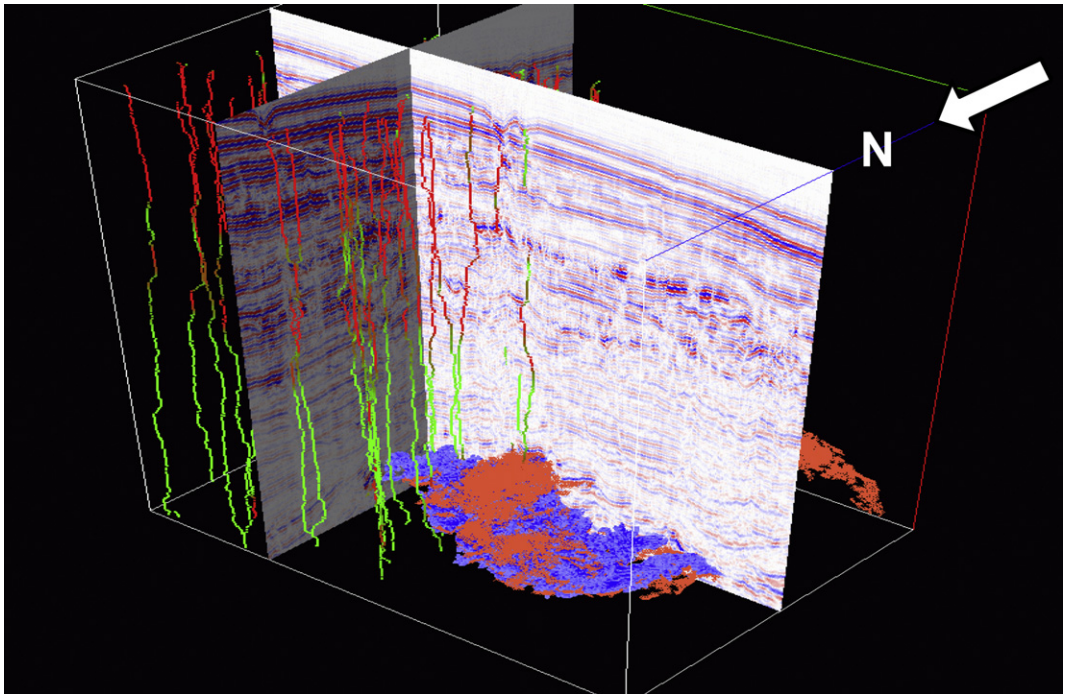

Fig. 8. 3D-visualisation of assumed reservoir units at the base (bright amplitude reflections, peak = blue and trough = red) and the pipes (green and red reflects high and low coherency, respectively). Note that the pipes cut in and out of vertical seismic sections.

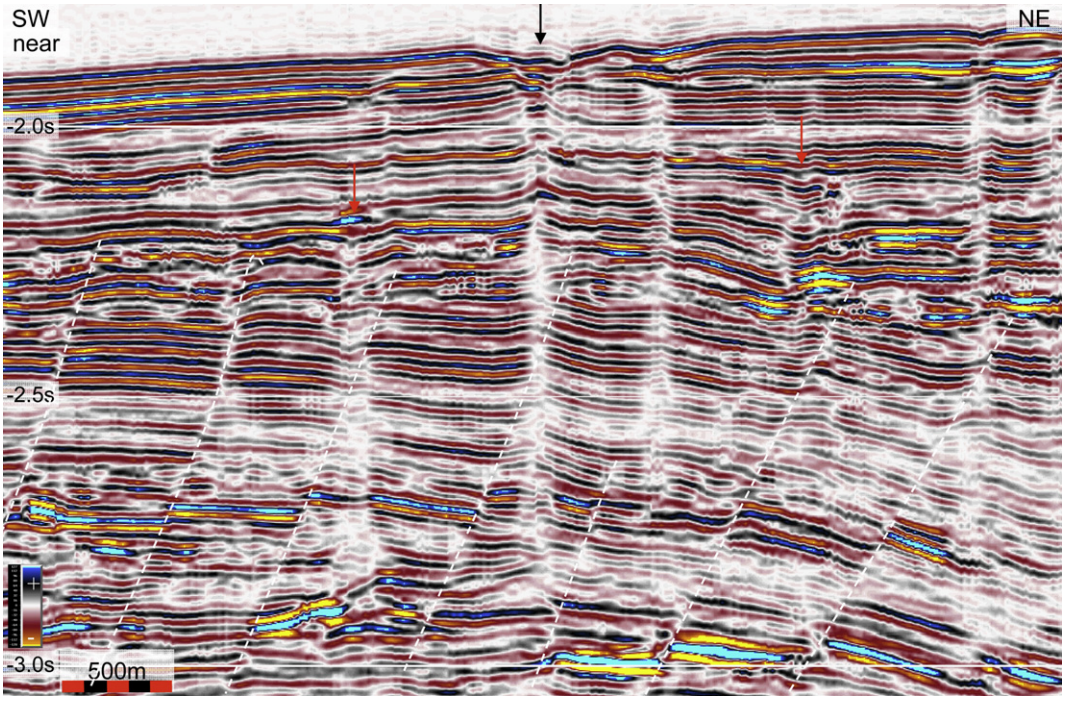

Fig. 9. The seismic pipe anomaly can be traced from the seafloor crater (black arrow) down to 2.8 s. It appears to cut across the fault (white dotted line). The red arrows point to the interpreted palaeo-seafloor craters with underlying pipe anomalies. The most south-westerly of the pipe anomalies appears to cut a fault and terminates in a bright anomaly.

to the core, to 0.5 m in the outermost parts. The concentric fracture pattern exposed in plane view extends upwards in the Lindos Bay clay but dies out downwards in the Kolymbia limestone. No slickensides are observed on these fractures. Most of the core-fill in the pipe has been removed by recent coastal erosion but the remaining part resembles the clay and clay clasts found in the underlying cavities in the reservoir.

3) Highest: Four exposures of blow-out pipes occur in the stratigraphically highest portion of the preserved Lindos Bay clay (cap rock), approximately 15 m above the top of the reservoir (Fig. 11). One of the pipes was analysed (Fig. 14). It comprises a central 70 cm wide central zone which upon digging was-found to contain angular clay clasts with no preferred structures and a black coating. The clasts in the central part were slightly

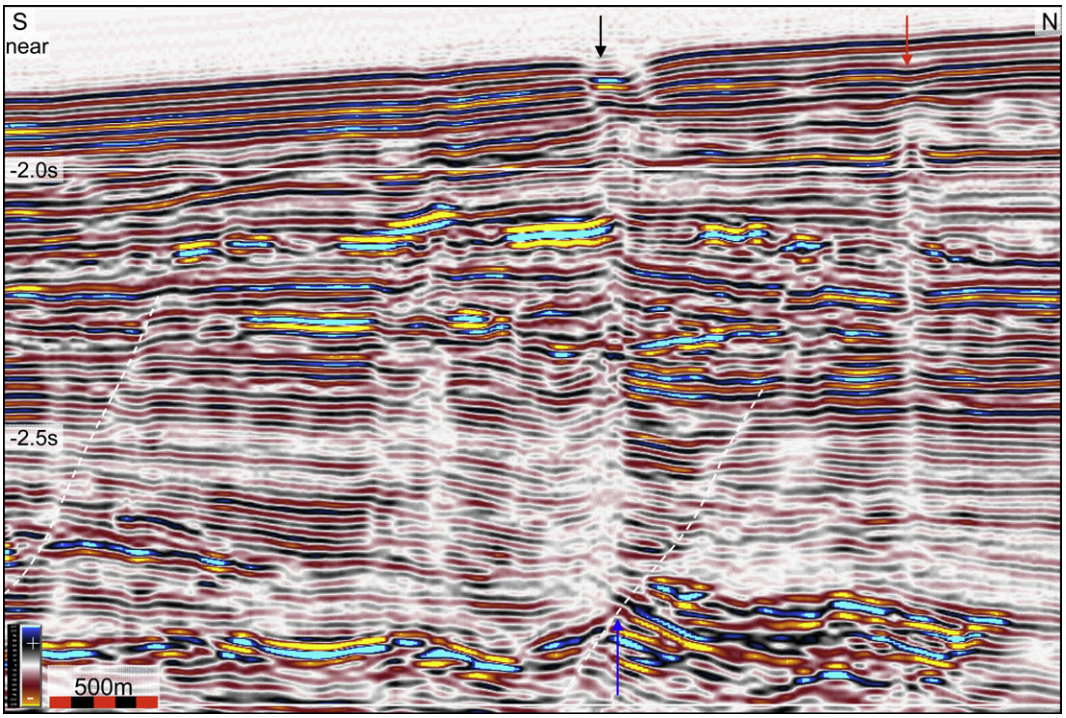

Fig. 10. The seismic pipe anomaly can be traced from the seafloor crater (black arrow) down to bright amplitudes at 2.8 s which is interpreted as a deep marine sandy reservoir. Note that the fault (white dotted line) intersects the bright amplitudes at the interpreted root of the pipe. The red arrow points to the interpreted palaeo-seafloor crater to the underlying pipe anomaly. Also this pipe may have a root in the same bright anomaly but the lower part of the pipe is diffusely expressed on seismic data.

Fig. 11. Simplified stratigraphy and picture of the study area at Cape Vagia, Rhodes. The stratigraphic position and location of the pipe-related observations numbered 1–3 are shown in Figures 12–14, respectively. The Haraki Limestone (H), Kolymbia Limestone and Lidos Bay clay of the Rhodes Formation lies unconformably on top of metamorphosed limestone basement.

larger (up to 5–10 cm) than those at the flank (<5 cm). The central pipe is rimmed by a 20 cm wide heavily sheared and foliated country rock and an outer approx. 4 m gradually less fractured zone. The 20 cm thick concentric fracture zone, which encloses the core, dips at an angle of ~60°–70° away from the core zone. Slickensides were frequently observed in the outer fractured zone. The transition between the core and the side was set at the first occurrence of foliated rocks. The fractures outside the 20 cm strongly foliated rim differ from those at the base of the Lindos Bay clay by being much more irregular and having slickensides. A simplified sketch of the pipe was drawn based on the observations (Fig. 15).

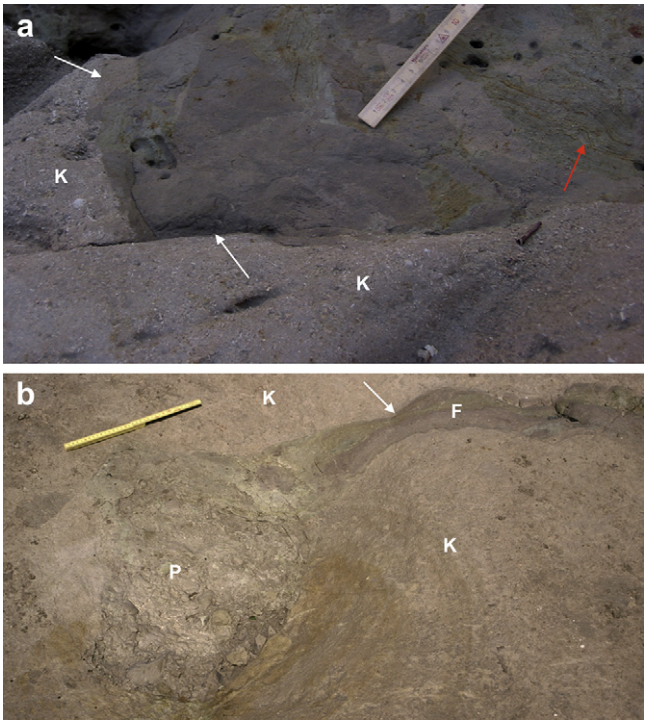

Fig. 12. a) The Kolymbia Limestone (K) has cavities which were filled with a breccia comprising clay clasts from the overlying Lindos Bay clay floating in a mud slurry matrix. Some of the clay clasts are deformed (red arrow). The boundary between the Kolymbia Limestone and breccia is sharp (white arrows). b) Some of the filled cavities have a circular pipe-shape (P) and are connected to other circular cavities through fractures (F). The yellow ruler is 35 cm long. Location 1 in Figure 11.

3.1. Seafloor crater at Tordis

A semi-circular crater, 7 m deep and 40 m wide, was observed on the seafloor close to the Tordis Field in the Norwegian North Sea (Fig. 16). This crater is interesting in relation to the pipe anomalies and associated seafloor craters offshore Nigeria because here the man-made formation process is known. Waste water was injected at pressure above lithostatic pressure in the upper part of the Hordaland Group, approximately 900 m below the seabed, with the intention of storing it in the overlying sands. Accidentally, the waste water reached the seafloor, which is located at a depth of 200 m. Pressure profiles from the injection well show a stepwise fracturing of the overburden. The injection lasted for approximately 5.5 months, at average rates of approximately 7000 m^3 a day, while the leakage to seafloor may have lasted for at least 16 days and possibly as long as 77 days. The seafloor crater is located 300 m east of the injection point. This event shows that water flowing through hydro fractures can develop large seafloor craters. It took between 150 000 m^3 and 550 000 m^3 of injected waste water to form the 7 m deep and 40 m wide seafloor crater. In relation to the pipe anomalies offshore Nigeria this demonstrated that:

- Relatively large blow-out craters can form during a relatively short time.
- Hydro fractures terminate in crater blow-out even though the state of stress is $\sigma1 > \sigma2 > \sigma3$.
- The seafloor crater is located 300 m laterally from the injection point, showing that the 900 m high water generated fracture conduit also has a lateral component.

4. Seismic modelling of vertical pipes

Seismic modelling was carried out to investigate how pipe structures like those found on Rhodes (Fig. 15) would appear on seismic data. The model had numerous nearly horizontal stratigraphic layers outside the pipe and a structureless material inside the pipe (Fig. 17). The model was up-scaled to contain a pipe 50 m wide and 1000 m deep. The material inside the pipe was varied with different contrasts in acoustic impedance between the inside and the outside of the pipe as shown in Figure 17a, c and e. Synthetic seismic data with a marine acquisition geometry were then generated by using an acoustic finite-difference method (Holberg, 1987). The seismic source was a Ricker wavelet with a centre frequency of 25 Hz, and a shot distance of 25 m. The distance between the receivers was 10 m, with a maximum offset of 4 km. A total of 600

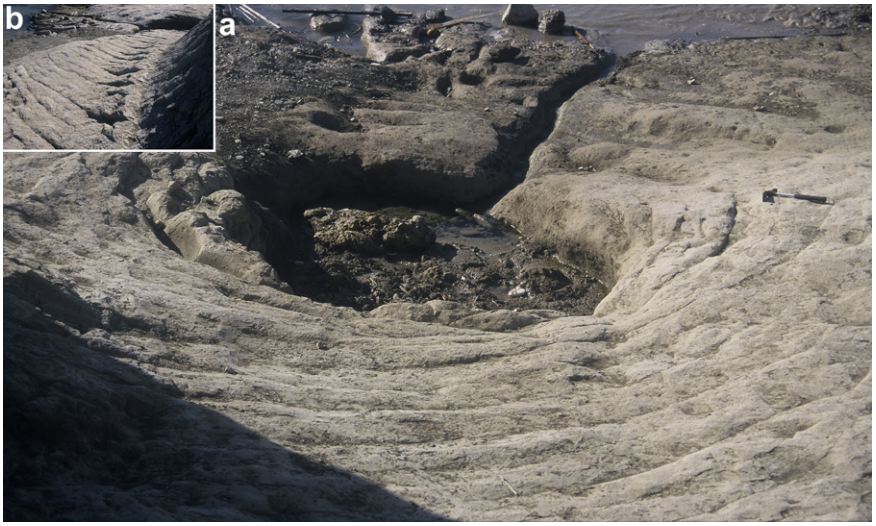

Fig. 13. Exposure of a circular pipe and the surrounding fractures in the lowermost part of the Lindos Bay clay, just above the Kolymbia limestone. The spacing of the circular fractures decreases towards the core of the pipe (b). No slickensides were observed on these fractures which therefore were interpreted as post-pipe contraction fractures. Location 2 in Figure 11.

shots were generated. Figure 17 shows only a small portion of the full model that was used to generate the synthetic data. Processing of the recorded data was limited to a mute of the direct arrival followed by shot-profile migration using a Split-step Fourier algorithm (Stoffa et al., 1990). No attempts were made to remove multiples and the velocity model utilised for the finite-difference modelling was also used for the migration. Figure 17b, d and f present parts of the resulting seismic sections corresponding to Figure 17a, c and e. The

Fig. 14. a) The exposed pipe structure in the upper part of the Lindos Bay clay (location 3 in Fig. 11). The yellow measuring tape is 60 cm long. The rim of the pipe (b) is strongly sheared. When the centre of the pipe (c) was dug out it comprised angular clasts with black coating. The fractures surrounding the pipe commonly have slickensides (d).

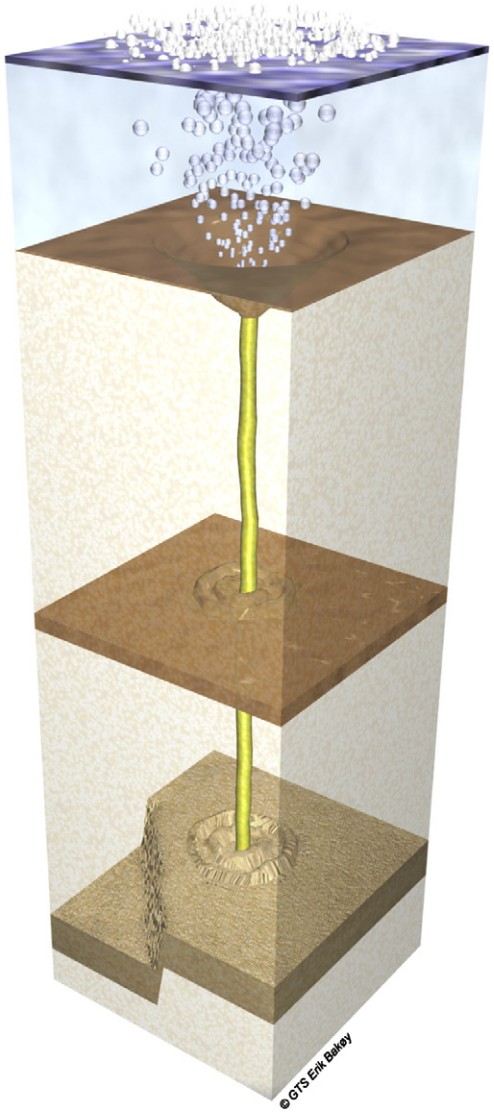

Fig. 15. Sketch of a typical pipe from the Niger study area, drawn on the basis of the observations in the pipe outcrops on Rhodes.

pipe is clearly visible, but due to the vertical geometry there is no image of the pipe itself, with the exception of the top (and bottom of Fig. 17b) which shows clear reflections. The pipe is thus only visible as a disruption of the surrounding layered sequence, but the termination of the reflectors against the vertical wall of the pipe will generate diffractions that are visible as hyperbolas on unmigrated data. In principle these hyperbolas will be collapsed to a point when the seismic data are migrated, but in practice the diffraction points will be smeared because of the limited frequency range of seismic data and the limited length of the recording cable. Because the width of the pipe is much less than the wavelength of the seismic waves, diffraction points on each side of the pipe will merge and appear as an apparent reflector segment within the pipe. This is illustrated in Figure 17g and h where the image of a pipe with a width much larger than the seismic wavelength does not show any sign of apparent internal reflectors. For real seismic data imperfect knowledge of the seismic velocity field will also contribute to smearing the diffraction points.

The modelled seismic picture resembles observations from seismic data from Nigeria where the pipes are represented by stacked central segments of reversed polarity (Fig. 18). According to the modelling these segments of reversed polarity inside the pipes are artefacts and do not represent any internal structures in the pipes. The modelled pipe with high acoustic impedance contrast with the surrounding layered sediments has pipe-like artefacts below the actual base of the pipe (Fig. 17b). No artefacts can be observed below the base of the pipe where the contrast is small (Fig. 17d and f).

5. Discussion

The pipe anomalies and associated seafloor craters observed on seismic data from offshore Nigeria are discussed with the insight gained from outcrop observations, seismic modelling and other relevant information. A formation model is suggested.

The pipe outcrops from Rhodes prove that vertical pipes form in relatively soft clays (Figs. 11–14). Seismic modelling of an up-scaled 50 m wide pipe, which is filled with structureless material, proves to be similar to the seismic pipe anomalies offshore Nigeria (Fig. 18). The processed seismic images of the pipe-model reveal geophysical artefacts within the pipe, at its flanks, and partly below it (Fig. 17). From the modelling we learn that the most accurate interpretation of the pipe boundary is at the transition from the continuous layer reflections outside and the disturbed seismic pattern inside the pipe. Layered reflections inside the pipe are geophysical artefacts in the model and we interpret similar reflections in the pipe anomalies offshore Nigeria to also be geophysical artefacts. The pipe-fill in the pipes offshore Nigeria may therefore be structureless as observed in the outcrops on Rhodes. Also, the small anticline anomalies in the position of the pipe are interpreted as geophysical artefacts (Figs. 4–6). Modelling proves that the base of the pipe is satisfactorily imaged where the acoustic impedance contrast with the surrounding sediments is small but that pipe-like multiples form below the base of the pipe if the acoustic impedance contrast is large (Fig. 17).

Even though the seismic anomalies found offshore Nigeria are significantly larger than those observed on Rhodes, their shape and form are similar. The outcrops of the pipes on Rhodes are typically between one and two orders of magnitude smaller than the seismically mapped pipes offshore Nigeria. Similar scale variations are observed in volcanic diatremes and maars. Lorenz (1986) discussed craters (maars) and associated feeder pipes (diatremes) formed by magma-heated steam. Volcanic maars have diameters from less than 100 m to over 1500 m and depths from tens of metres to 200 m. The depth of diatremes from the surface to the root zone is unknown but may reach 2000 m–2500 m. All observations of historically active maars were short-lived (3 to 8 days duration) and they produced rather small maars (170 m–320 m in diameter) (Lorenz, 1986). The crater with the largest maars was active for the longest period of time, suggesting that the longer duration, the larger the maars. The size variations of the volcanic maars slightly exceed one order of magnitude while the size difference between the observations on Rhodes and Nigeria are less than two orders of magnitude. The exact number is difficult to estimate as the upper part of the Lindos Bay clay was eroded and the primary length of the Rhodes pipes is unknown. The relative large size range of related volcanic structures suggests that maars and diatremes can form under a variety of physical conditions. A similar range in sizes may exist for pipes formed in soft sediments and the pipe anomalies offshore Nigeria may therefore represent larger scale versions of the vertical pipes on Rhodes.

5.1. Formation processes

In common with the pipe outcrops on Rhodes, the interpreted pipes offshore Nigeria can be traced down to a reservoir unit. The

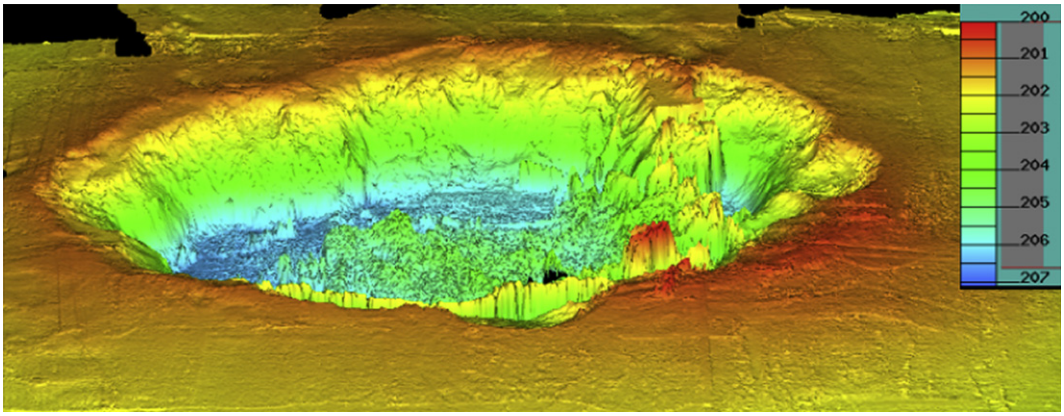

Fig. 16. Semi-circular seafloor crater above the Tordis Field in the Norwegian North Sea. The crater is 40 m wide and 7 m deep. Water depth scale (m) is given. The crater was formed when injection water accidentally escaped to the seafloor.

pressure in the water, oil and/or gas occupying the reservoir pore space must have been high enough to hydro fracture the overburden. The development of the man-made seafloor crater above the Tordis Field demonstrates that hydro fractures formed by incompressible water can develop through repeated episodes of fluid pressure build-ups. For each growth increment during such stepwise and gradual fracturing process the overpressured fluid will migrate to a larger rock volume before hydro fracturing at the weakest point. As in the Tordis case, the final fluid conduit route does not have to be vertical.

If, on the other hand, gas occupied the pores in the reservoir, the pressure history would be different inside the growing hydro fracture. Gas is compressible and the pressure drop due to the fracture volume increase would be small. The gas pressure in the propagating vertical fracture would therefore be only slightly reduced as the hydro fracture climbed upwards through the cap rock. The gas pressure at the upper tip of the hydro fracture would easily remain in excess of the overburden stress plus the tensile strength in the rocks. A fast, almost explosive, propagation of the hydro fracture is likely. The strongly sheared flank of the pipes on Rhodes and associated fractures with slickensides give evidence of brittle deformation associated with the pipe formation (Fig. 14). In order to deform such soft sediments in a brittle manner the strain rate must have been high.

The observed pipe anomalies offshore Nigeria appear to be close to vertical. They are interpreted to cut through fault zones and locally through overlying interpreted sandy intervals (Figs. 9 and 10). We expect that a stepwise water- or oil-supported fracture propagation would follow weakness zones as fault planes and have a more irregular propagation track. As for the Tordis case such conduits are not likely to be vertical. Since all the pipes are almost vertical we suggest that gas rather than water or oil was a significant part of the reservoir fluid when the pipes formed. When a gas-filled hydro fracture established a fracture connection from the reservoir to the surface a violent gas flow would take place. Such flow could erode and deform the sides of the hydro fracture to form a pipe.

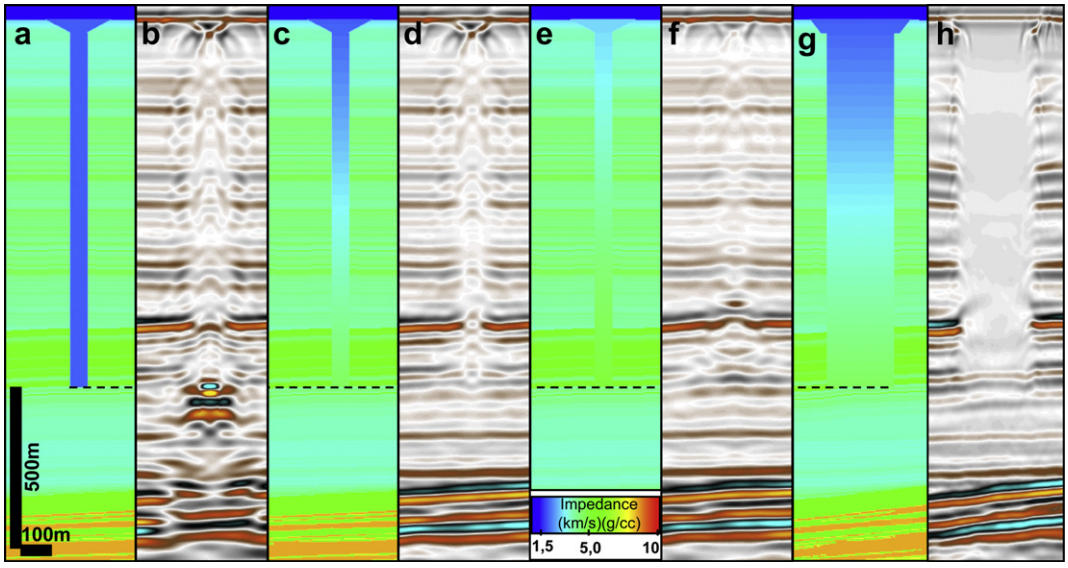

Fig. 17. Figure 17a, c and e shows parts of a layered acoustic model from Johansen et al. (2007) with a 50 wide (150 m at seafloor) and 1 km deep pipe comprising structureless material. The acoustic impedance in the material inside the pipe is constant in a), gradual increasing to depth in c), e), and g). Synthetic seismic data of models Figure 17a, c and e are shown in Figure 17b, d and f, respectively. The pipe is clearly visible as a disruption of the surrounding layered sequence on the seismic data in all models, but due to the vertical geometry there is no image of the pipe itself, with the exception of the top (and bottom of Fig. 17b) which shows clear reflections. Notice the multiples and distortions below the base of the pipe in Figure 17b (dotted line is drawn at the base of the pipe). There is a significant change in expression of the lower part of the intra-pipe reflections from Figure 17d and f where the acoustic impedance is slightly lower and higher than the surrounding layered material. A 500 m wide pipe was modelled to show that the artefacts at the pipe boundary do not extending throughout the interior of the pipe if the width of the pipe is larger than the dominating seismic wavelength, which in our case is approximately 100 m (Fig. 17g and h).

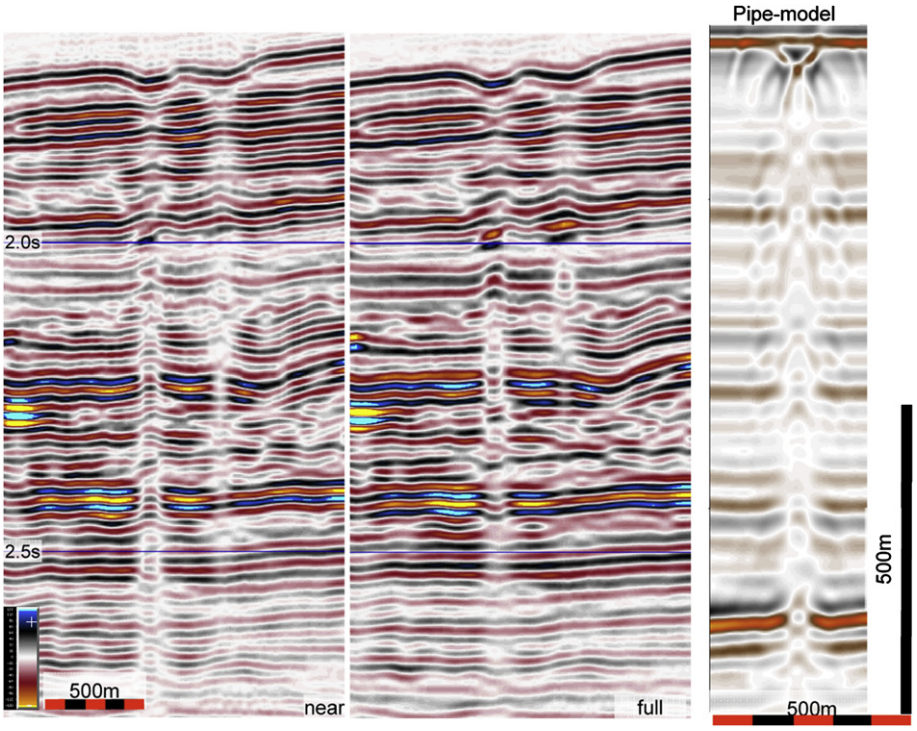

Fig. 18. Comparison between the near and full stack processed pipe anomalies from offshore Nigeria and full stack processed data from the seismic modelled 50 m wide pipe. The vertical scale is similar but the horizontal scale of the pipe-model is twice that of the Nigeria seismic sections.

The cause of the high fluid pressure may be any of those discussed in the literature (Boehm and Moore, 2002; Reilly and Flemings, 2010; Sahagian and Proussevitch, 1992; Seldon and Flemings, 2005; Swarbrick et al., 2002). We do not wish to speculate too much on this aspect but note that there is sound evidence that the underlying large-scale detachment faults glide on an overpressured layer (Cobbold et al., 2009). High pressure fluids may have reached shallow reservoirs both through the active thrust fault in the northern part of the study area and the left-lateral strike-slip fault below the pipe anomaly cluster off Nigeria.

5.2. Duration and termination of blow-out

Historical data from volcanic maars show short episodes of activity, i.e., 3–8 days (Lorenz, 1986). The 40 m wide seafloor crater above the Tordis Field developed due to water flow to seafloor in a period of between 16 and 77 days. Simple pore volume calculations of the assumed sand reservoir bodies below the pipes off Nigeria suggest that pipes 1 m–50 m wide could empty the reservoir in a period ranging from less than a few months to an hour. Assuming that the interpreted width of pipes are correct (50 m–150 m) (Fig. 6), we speculate that the main gas blow-out from a pipe offshore Nigeria was short-lived (hours to a few weeks). When the pore fluid pressure dropped below the weight of the gas–water sediments slurry in the pipe the blow-out must have terminated. The outcrop study from Rhodes has demonstrated that the cavities in the reservoir and pipes were plugged by a mixture of blocks derived from the sidewalls and water–mud slurry at the end of the blow-out. Similar plugging may have taken place in the pipes offshore Nigeria and prevented easy reuse of old pipes. This may explain why approximately 110 large craters with underlying pipes have formed in the study area and the 41 pipe-related structures on Rhodes. Figure 19

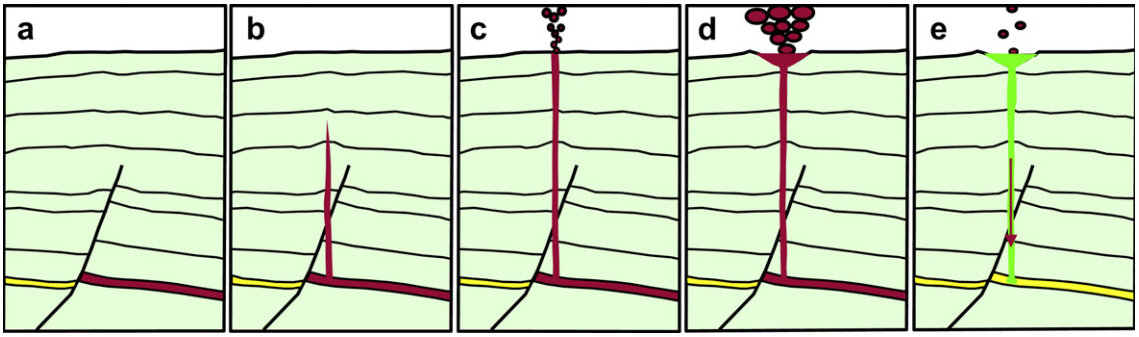

Fig. 19. Schematic illustration of the formation and evolution of a blow-out pipe. a) The fluid pressure in the reservoir 1000 m below seafloor increases. b) The fluid pressure overcomes the overburden stress plus the tensile strength of the cap rock and a hydro fracture propagates upward through the overburden. Since compressible gas is a major part of the fluid, the fracture fluid pressure remains high during the propagation. c) When the hydro fracture reaches the seafloor a high speed fluid flow conduit is established between the reservoir and the seafloor. d) Gas, fluid and rock fragments flow at high speed through the fracture and erode and shear the side of the hydro fracture to form a pipe structure. A crater develops on the seafloor. Gas blows continues from hours to a few weeks. The high speed fluid flow causes sand production and a cavity forms in the reservoir. e) The blow-out terminates when the pore fluid pressure drops below the weight of the gas–water sediments slurry in the pipe. The slurry falls back into the pipe and plugs the cavity in the reservoir and the pipe. This plugging prevents the formation of new pipes at the same location and explains the large numbers of pipes.

sums up our preferred formation model for the pipes offshore Nigeria.

6. Conclusion

Approximately 110 large seafloor craters (from 100 m to 700 m in diameter) are clustered in a 60 km^2 area above structural closure offshore Nigeria. Cones (~60 m deep) are interpreted below many of the craters and vertical pipe anomalies with a distorted seismic signal below them. The pipes can be traced 1000 m–1300 m below the seafloor into interpreted sandy reservoir zones. The structures are interpreted as vertical fracture pipes similar to, but much larger than those observed in outcrops on Rhodes.

Based on outcrop observation on Rhodes we constructed an acoustic model of a 50 m wide and 1000 m long pipe. Seismic modelling proved that such pipes would be imaged on seismic data, they are similar to the seismic pipe anomalies in Nigeria but also revealed that their seismic image is hampered by several geophysical artefacts.

A formation model for the pipes is suggested: High fluid pressure in the reservoir generated hydro fractures from the reservoir to the seafloor where high speed gas formed pipes, cones and seafloor craters. After hours to weeks of gas and fluid flow through the pipe the pore pressure in the reservoir was reduced and the blow-out terminated. A clast-filled muddy slurry fell back into the pipe and plugged the cavity in the reservoir and the pipe which prevented reuse.

Acknowledgments

We are grateful to Statoil for funding the research and allowing us to publish the results. We also will thank Nigerian National Petroleum Corporation, Texaco and Statoil for permission to publish the seismic sections. Two anonymous reviewers gave critical comments that improved the manuscript. We are grateful to Stewart Clark, Norwegian University of Science and Technology for his language help.

References

Arntsen, B., Wensaas, L., Løseth, H., Hermanrud, C., 2007. Seismic modelling of gas chimneys. Geophysics 72, 251–259.

Boehm, A., Moore, J.C., 2002. Fluidized sandstone intrusions as an indicator of Paleostress orientation, Santa Cruz, California. Geofluids 2, 147–161.

Bünz, S., Mienert, J., Berndt, C., 2003. Geological controls on the Storegga gas-hydrate system of the mid-Norwegian continental margin. Earth and Planetary Science Letters 209, 291–307.

Cartwright, J., Huuse, M., Aplin, A., 2007. Seal bypass system. AAPG Bulletin 91, 1141–1166.

Cobbold, P.R., Diraison, M., Rossello, E.A., 1999. Bitumen veins and Eocene transpression, Neuquén Basin, Argentina. Tectonophysics 314, 423–442.

Cobbold, P.R., Clarke, B.J., Løseth, H., 2009. Structural consequences of fluid overpressure and seepage forces in the outer thrust belt of the Niger Delta. Petroleum Geoscience 15, 3–15.

Cornée, J.J., Moissette, P., Joannin, S., Suc, J.P., Quillévéré, F., Krijgsman, W., Hilgen, F., Koskeridou, E., Münch, P., Lécuyer, C., Desvignes, P., 2006a. Tectonic and climatic controls on coastal sedimentation: the late Pliocene–Middle Pleistocene of northeastern Rhodes, Greece. Sedimentary Geology 187, 159–181.

Cornée, J.J., Münch, P., Quillévéré, F., Moissette, P., Vasiliev, I., Krijgsman, W., Verati, C., Lécuyer, C., 2006b. Timing of Late Pliocene to Middle Pleistocene tectonic events in Rhodes (Greece) inferred from magneto-biostratigraphy and 40Ar/39Ar dating of a volcaniclastic layer. Earth and Planetary Science Letters 250, 281–291.

Deville, E., Guerlais, S.-H., Callec, Y., Griboulard, R., Huyghe, P., Lallemant, S., Mascle, A., Noble, M., Schmitz, J., The Collaboration Of The Caramba Working Group, 2006. Liquefied vs stratified sediment mobilization processes: insight from the South of the Barbados accretionary prism. Tectonophysics 428, 33–47.

Deville, E., Mascle, A., in press. The Barbados ridge: a mature accretionary wedge in front of the lesser Antilles active margin. In: Bally, A.W., Roberts, D.G. (Eds.), Principles of Regional Geology. Elsevier.

Doust, H., Omatsola, E., 1989. Niger Delta. In: Edwards, J.D., Santogrossi, P.A. (Eds.), Divergent/Passive Margin Basins, 48. American Association of Petroleum Geologists Memoir, pp. 201–238.

Evans, R.J., Stewart, S.A., Davies, R.J., 2008. The structure and formation of mud volcano summit calderas. Journal of the Geological Society 165, 769–780.

Graue, K., 2000. Mud volcanoes in deepwater Nigeria. Marine and Petroleum Geology 17, 959–974.

Haack, R.C., Sundararaman, P., Diedjomahor, J.O., Xiao, H., Gant, N.J., May, E.D., Kelsch, K., 2000. Niger Delta petroleum systems, Nigeria. In: Mello, M.R., Katz, B.J. (Eds.), Petroleum Systems of South Atlantic Margins. American Association of Petroleum Geologists Memoir, vol. 73, pp. 213–232.

Hall, J., Aksu, A.E., Yaltırak, C., Winsor, J.D., 2009. Structural architecture of the Rhodes Basin: a deep depocentre that evolved since the Pliocene at the junction of Hellenic and Cyprus Arcs, eastern Mediterranean. Marine Geology 258, 1–23.

Hanken, N.M., Bromley, R.G., Miller, J., 1996. Plio–Pleistocene sediments in coastal grabens, north-east Rhodes, Greece. Geological Journal 31, 271–298.

Heggland R., Nygaard E., 1998. Shale intrusions and associated surface expressions – examples from Nigerian and Norwegian deepwater areas. Offshore technology conference 1998, OTC 8641.

Holberg, O., 1987. Computational aspects of the choice of operator and sampling interval for numerical differentiation in large-scale simulation of wave phenomena. Geophysical Prospecting 37, 629–655.

Hovland, M., Judd, A.G., 1988. Seabed Pockmarks and Seepages. Impact on Geology, Biology and the Marine Environment. Graham and Trotman Ltd., London, 293 pp.

Hustoft, S., Bünz, S., Mienert, J., 2010. Three-dimensional seismic analysis of the morphology and spatial distribution of chimneys beneath the Nyegga pockmark field, offshore mid-Norway. Basin Research 22, 465–480. doi:10.1111/j.1365-2117.2010.00486.x.

Hustoft, S., Mienert, J., Bünz, S., Nouzé, H., 2007. High-resolution 3D-seismic data indicate focussed fluid migration pathways above polygonal fault systems of the mid-Norwegian margin. Marine Geology 245, 89–106.

Johansen, S., Granberg, E., Mellere, D., Arntsen, B., Olsen, T., 2007. Decoupling of seismic reflectors and stratigraphic timelines: A modeling study of Tertiary strata from Svalbard. Geophysics 72, SM273–SM280.

Leifer, I., Luyendyk, B.P., Boles, J., Clark, J.F., 2006. Natural marine seepage blowout: contribution to atmospheric methane. Global Biogeochemical Cycles 20, GB3008.

Lorenz, V., 1986. On the growth of maars and diatremes and its relevance to the formation of tuff rings. Bulletin of Volcanology 48, 265–274.

Løseth, H., Wensaas, L., Arntsen, B., Hanken, N., Basire, C., Graue, K., 2001. 1000 m long gas blow out pipes. 63rd EAGE Conference and Exhibition, Extended abstract, 524–527.

Løseth, H., Gading, M., Wensaas, L., 2009. Hydrocarbon leakage interpreted on seismic data. Marine and Petroleum Geology 26, 1304–1319.

Løvlie, R., Hanken, N.M., 2002. Conglomerate test of non-lithified Plio–Pleistocene marine sediments suggests pDRM type remagnetisation. Physics and Chemistry of the Earth 27, 1121–1130.

Mazzinia, A., Ivanovb, M.K., Nermoena, A., Bahrc, A., Bohrmannc, G., Svensena, H., Planke, S., 2008. Complex plumbing systems in the near subsurface: geometries of authigenic carbonates from Dolgovskoy Mound (Black Sea) constrained by analogue experiments. Marine and Petroleum Geology 25, 457–472.

Morgan, R., 2003. Prospectivity in ultradeep water: the case for petroleum generation and migration within the outer parts of the Niger Delta apron. In: Arthur, T.J., McGregor, D.S., Cameron, N.R. (Eds.), Petroleum Geology of Africa: New Themes and Developing Technologies, 207. Geological Society, London, pp. 151–164. Special Publications.

Moss, J.L., Cartwright, J.A., 2010a. The spatial and temporal distribution of pipe formation, offshore Namibia. Marine and Petroleum Geology 27, 1216–1234. doi:10.1016/j.marpetgeo.2009.12.013.

Moss, J., Cartwright, J.A., 2010b. 3D seismic expression of km-scale fluid escape pipes from offshore Namibia. Basin Research 22, 481–501. doi:10.1111/j.1365-2117.2010.00461.x.

Parnell, J., Kelly, J., 2003. Remobilization of sand from consolidated sandstones: evidence from mixed bitumen-sand intrusions. In: Van Rensbergen, P., Hillis, R.R., Maltman, A.J., Morley, C.K. (Eds.), Subsurface Sediment Mobilization. Geological Society, 216. Geological Society, London, pp. 505–513. Special Publications.

Reilly, M., Flemings, P.B., 2010. Deep pore pressures and seafloor venting in the auger basin, Gulf of Mexico. Basin Research 22, 380–397. doi:10.1111/j.1365-2117.2010.00481.x.

Revil, A., Cathles, L.M., 2002. Fluid transport by solitary waves along growing faults – A field example from the South Eugene Island Basin, Gulf of Mexico. Earth and Planetary Science Letters 202, 321–335.

Rodrigues, N., Cobbold, P.R., Løseth, H., 2009. Physical modelling of sand injectites. Tectonophysics 474, 610–632.

Sahagian, D.L., Proussevitch, A.A., 1992. Bubbles in volcanic systems. Nature 359, 485.

Seldon, B., Flemmings, P.B., 2005. Reservoir pressure and seafloor venting: Predicting trap integrity in a Gulf of Mexico deepwater turbidite minibasin. AAPG Bulletin 89, 193–209.

Stoffa, P.L., Fokkema, J., Freire, R.M.L., Kessinger, W.P., 1990. Split-step Fourier migration. Geophysics 55, 410–421.

Swarbrick, R.E., Osborne, M.J., Yardley, G.S., 2002. Comparison of overpressure magnitude resulting from the main generating mechanisms. In: Huffman, A.R., Bowers, G.L. (Eds.), Pressure Regimes in Sedimentary Basins and Their Prediction, 76. American Association of Petroleum Geologists Memoir, pp. 1–12.

Trincardi, F., Cattaneo, A., Correggiari, A., Ridente, D., 2004. Evidence of soft sediment deformation, fluid escape, sediment failure and regional weak layers within the late Quaternary mud deposits of the Adriatic Sea. Marine Geology 213, 91–119.